



Published in final edited form as:

J Invest Dermatol. 2019 December ; 139(12): 2447–2457.e7. doi:10.1016/j.jid.2019.04.023.

Quantitative Trait Locus and Integrative Genomics Revealed Candidate Modifier Genes for Ectopic Mineralization in Mouse Models of Pseudoxanthoma Elasticum

Qiaoli Li¹, Vivek M. Philip², Timothy M. Stearns², Jason A. Bubier², Benjamin L. King³, Benjamin E. Low², Michael V. Wiles², Amir Hossein Saeidian^{1,4}, Beth A. Sundberg², Jouni Uitto¹, John P. Sundberg²

¹Department of Dermatology and Cutaneous Biology and the Jefferson Institute of Molecular Medicine, Sidney Kimmel Medical College, and the PXE International Center of Excellence in Research and Clinical Care, Thomas Jefferson University, Philadelphia, PA

²The Jackson Laboratory, Bar Harbor, ME

³Department of Molecular and Biomedical Sciences, University of Maine, Orono, ME

⁴Genetics, Genomics and Cancer Biology PhD Program, Thomas Jefferson University, Philadelphia, PA

Abstract

Pseudoxanthoma elasticum (PXE), a prototype of heritable multi-system ectopic mineralization disorders, is caused by mutations in the *ABCC6* gene encoding a putative efflux transporter, ABCC6. The phenotypic spectrum of PXE varies, and the correlation between genotype and phenotype has not been established. To identify genetic modifiers, we performed quantitative trait locus analysis in inbred mouse strains that carry the same hypomorphic allele in *Abcc6* yet with highly variable ectopic mineralization phenotypes of PXE. *Abcc6* was confirmed as a major determinant for ectopic mineralization in multiple tissues. Integrative analysis using functional genomics tools that included GeneWeaver, String, and Mouse Genome Informatics identified a total of nine additional candidate modifier genes that could influence the organ-specific ectopic mineralization phenotypes. Integration of the candidate genes into the existing ectopic

Corresponding author: Qiaoli Li, PhD, Department of Dermatology and Cutaneous Biology, Sidney Kimmel Medical College, PXE International Center of Excellence in Research and Clinical Care, Thomas Jefferson University, 233 S. 10th Street, Suite 431 BLSB, Philadelphia, Pennsylvania 19107, Qiaoli.Li@jefferson.edu.

AUTHOR CONTRIBUTIONS

QL, JU, and JPS designed the study. QL and JPS performed the experiments. QL, VMP, TMS, JAB, BLK, BEL, MVW, AHS, and BAS did data analysis. QL and JPS drafted the manuscript. All authors critically revised the manuscript.

Publisher's Disclaimer: This is a PDF file of an unedited manuscript that has been accepted for publication. As a service to our customers we are providing this early version of the manuscript. The manuscript will undergo copyediting, typesetting, and review of the resulting proof before it is published in its final citable form. Please note that during the production process errors may be discovered which could affect the content, and all legal disclaimers that apply to the journal pertain.

CONFLICT OF INTEREST

JPS has or recently completed sponsored research projects with Biocon, Takeda, Theravance, and Curadim. JPS has a consulting agreement with Bioniz. All are unrelated to this project. All other investigators state no conflict of interest.

DATA AVAILABILITY STATEMENT

Not applicable. No datasets were generated.

mineralization gene network expands the current knowledge on the complexity of the network that as a whole governs ectopic mineralization in soft connective tissues.

Keywords

Pseudoxanthoma elasticum; ectopic mineralization; modifier genes; quantitative trait locus

INTRODUCTION

Ectopic mineralization of connective tissues is a complex process leading to deposition of calcium phosphate complexes in the extracellular matrix, particularly affecting the skin and the arterial blood vessels. Ectopic mineralization is a global pathological problem encountered in aging, cancer, diabetes, and autoimmune diseases, causing significant morbidity and mortality. Several Mendelian genetic disorders share phenotypic similarities with the acquired forms of ectopic mineralization, and serve as genetically controlled model systems to study various facets of pathological mineralization (Nitschke and Rutsch, 2012). Pseudoxanthoma elasticum (PXE; OMIM#264800), a multi-system disorder clinically affecting the skin, eyes, and the cardiovascular system, is characterized by late-onset and slowly progressive connective tissue mineralization (Neldner, 1988; Uitto *et al.*, 2017; Li *et al.*, 2019). PXE is an autosomal recessive disorder with complete penetrance, a slight female preponderance, and prevalence in the 1 in 50,000–70,000 range. The phenotypic spectrum is highly variable with inter- and intra-familial heterogeneity in the age at onset and the extent and severity of organ system involvement, adding to the diagnostic difficulty.

Identification of mutations in the ATP-binding cassette, subfamily C, member 6 (*ABCC6*) gene, as the primary genetic basis of PXE, was accomplished in 2000 (Ringpfeil *et al.*, 2000; Le Saux *et al.*, 2000; Bergen *et al.*, 2000). Since then, tremendous progress has been made in understanding the molecular genetics, spectrum of clinical phenotypes, and pathogenesis of this disease (Uitto *et al.*, 2017; Li *et al.*, 2019). The *ABCC6* gene encodes the transmembrane ABCC6 protein, a putative efflux transporter (Cai *et al.*, 2002; Ilias *et al.*, 2002; Borst *et al.*, 2019), expressed primarily in the liver (Belinsky and Kruh, 1999; Scheffer *et al.*, 2002). PXE was determined in murine models to be a metabolic disorder caused by defective ABCC6 transporter activity leading to ectopic mineralization in soft connective tissues (Jiang *et al.*, 2009; Jiang *et al.*, 2010; Li *et al.*, 2017).

Over 400 distinct mutations in *ABCC6* have been reported in PXE patients ([https://www.ncbi.nlm.nih.gov/clinvar/?term=abcc6\[gene\]](https://www.ncbi.nlm.nih.gov/clinvar/?term=abcc6[gene])). However, no correlation could be established between the phenotype and the nature or the position of the mutations in *ABCC6* (Pfundner *et al.*, 2007; Iwanaga *et al.*, 2017; Legrand *et al.*, 2017). Evidence has emerged suggesting the presence of modifier genes for PXE (Dabisch-Ruthe *et al.*, 2014; Li *et al.*, 2009b). Adding to the genetic complexity of PXE, recent findings revealed that the same *ABCC6* mutations can also cause type 2 generalized arterial calcification of infancy (GACI; OMIM#614473), a distinct clinical entity most often caused by *ENPP1* mutations (GACI; OMIM#208000), resulting in significant mortality in infancy due to early onset of extensive vascular mineralization (Rutsch *et al.*, 2003; Li *et al.*, 2014a; Nitschke *et al.*, 2012). In

addition, in an unusually severe vascular case presenting as GACI the patient died at 15 months of age while his older brother developed PXE in adolescence (Le Boulanger *et al.*, 2010). Presumably, the same *ABCC6* mutations in the family resulted in two ends of the clinical severity spectrum of ectopic mineralization. These observations indicate a substantial gap in our understanding of the genetic factors that modify disease severity.

Two *Abcc6*^{-/-} mouse models of PXE develop late onset, yet progressive, lesions similar to those seen in human patients with PXE (Klement *et al.*, 2005; Gorgels *et al.*, 2005). Spontaneous ectopic mineralization, at various degrees of severity, was also identified in four inbred mouse strains in a large-scale aging study consisting of 28 inbred strains of mice (Sundberg *et al.*, 2011; Berndt *et al.*, 2013). These strains, 129S1/SvImJ (129), C3H/HeJ (C3), DBA/2J (D2), and KK/HIJ (KK), harbor a non-synonymous coding SNP in the *Abcc6* gene (rs32756904) resulting in reduced ABCC6 protein levels in the liver, the primary site of expression of the gene (Li *et al.*, 2012). Among these four inbred strains, KK displayed the most severe multi-system mineralization phenotype similar to that in *Abcc6*^{-/-} mice, therefore providing another model of PXE (Li *et al.*, 2012). The 129 strain developed mineralization to a much lesser extent while C3 and D2 mice developed extremely mild mineralization. By contrast, B6 mice, wild type for the *Abcc6* allele, do not develop PXE-like lesions. As the aging study carefully maintained all the strains under the same environmental and high barrier conditions, the variability in severity of mineralization (quantitative difference) among these four strains with the same *Abcc6* allelic mutation, suggest that modifier genes regulate phenotypic presentation. To identify the modifier genes, crosses were carried out between KK and either B6 or D2 mice and from which a number of Quantitative Trait Loci (QTLs) for ectopic mineralization were identified. As expected, *Abcc6* was confirmed as a major player in ectopic mineralization in PXE. Integration of functional genomic data of these inbred strains revealed nine additional candidate modifier genes and provided insights into potential networks controlling ectopic mineralization.

RESULTS

Analysis of F1 hybrid phenotypes suggested recessive QTL for vibrissae mineralization, the hallmark of PXE in mice

Crosses of the severely affected KK mice with B6, a strain without mineralization, or with D2, a strain with mild PXE, were used in QTL analysis to localize genomic intervals that have effects on ectopic mineralization phenotype. Their respective F1 progeny, B6KKF1 and D2KKF1, were analyzed at 12 weeks of age. The severity of vibrissae mineralization in the muzzle skin, a hallmark of PXE in mice, was scored by semi-quantitative histopathological analysis (Figure 1a). In addition, the degree of mineralization in muzzle skin was quantified by an independent chemical assay of calcium. Linear regression analysis of log₂ transformed calcium content and severity score had an adjusted R² = 0.8957 for the parental B6, D2, KK, B6KKF1 and D2KKF1 mice (Figure S1), indicating the consistency between these two techniques to evaluate the degree of ectopic mineralization. As such, histologic severity scores were used in the study for muzzle skin and other organs. Severity scores of B6KKF1 and D2KKF1 were not significantly different than the B6 and D2 parental strain (ANOVA, F = 1.80, P = 0.1569), but were significantly different from KK (ANOVA, F = 150.75, P <

0.0001). These results suggest that recessive genes cause vibrissae mineralization observed in KK mice. F1 mice were backcrossed with the KK parental strain and N2 progeny, (B6KKF1)KK and (D2KKF1)KK, were generated.

Analysis of N2 hybrid phenotypes revealed various degrees of mineralization in multiple tissues (quantitative traits)

The N2 progeny consisting of a total of 183 (B6KKF1)KK mice and 191 (D2KKF1)KK were necropsied at 12 weeks of age. A number of organs known to be affected in PXE, including muzzle skin, heart, kidney, eyes, and lung, were collected for histologic evaluation of ectopic mineralization (Figures 1–3; Figures S2,S3). While there appears to be a slight female preponderance (1.3:1 Female:Male ratio) for PXE in humans (Neldner, 1988), there is no major sexual dichotomy in mice for the majority of the inbred and hybrid strains.

QTL analysis identified chromosome regions containing modifier genes

We identified 8 organ-specific QTLs for ectopic mineralization. These QTLs were designated as *Vmm1* to *Vmm8* and deposited in the Mouse Genome Database (MGD), a community database resource for laboratory mouse. These QTLs contain 73 to 1,203 genes at each locus, some of which overlap, that contribute to the PXE phenotype in multiple tissues (Table 1). When analyzed by lesion and organ, five of the QTLs were identified on Chr.7 in the KK and B6 cross but not in the KK and D2 cross (Figures 1–3; Figures S2,S3). Among them, *Vmm3* and *Vmm4* overlapped with *Abcc6* (position 46 Mbp on Chr.7) which resided in close proximity to *Vmm1*, *Vmm2*, and *Vmm6* (Table 1). Thus, the *Abcc6* gene was likely linked to the PXE phenotype in multiple organs, as expected. The remaining three QTLs, one for heart mineralization on Chr.3 (*Vmm7*) and two overlapping QTLs for kidney mineralization on Chr.5 (*Vmm5* and *Vmm8*), contain genes, yet to be identified, that modify ectopic mineralization in these tissues (Figures 2, 3).

Integrative analysis identified candidate modifier genes for PXE

GeneWeaver has been used successfully to identify candidate genes related to other phenotypes (Delprato *et al.*, 2017; Bubier *et al.*, 2014). Combination of the QTL intervals with transcriptome studies of organs, specifically heart (Lin *et al.*, 2014) and kidney (Rubin *et al.*, 2016) and presence of differential SNPs (coding and non-coding) between KK and B6/D2, the number of candidate modifier genes was reduced to 30 and 33 for *Vmm7* locus on Chr.3 and *Vmm5/Vmm8* loci on Chr.5, respectively (Figure 4a,b). We next performed functional genomics analysis to further narrow down the candidate gene list. The prioritization criteria includes the following: genes consistent with the ectopic mineralization phenotype in either human or mouse in prior studies, genes that interact with *Abcc6* at String database (Szkarczyk *et al.*, 2017), publicly available information at GeneWeaver and Mouse Genome Informatics including genes that alter bone mineralization and mineral homeostasis. A total of nine candidate genes were identified (Figure 4c). Among them, two candidate genes were identified for heart mineralization in the Chr.3 QTL in KK and D2 cross (Figure S4), and seven candidate genes fulfilled the selection criteria for kidney mineralization in the Chr.5 QTL in KK crosses with either B6 or D2 (Figure S5).

Generation and expansion of an ectopic mineralization gene network

To illustrate the complexity of ectopic mineralization gene network, 22 genes known to be involved in ectopic mineralization phenotypes in humans and/or in mice (Table S1) together with the nine candidate genes for modification of ectopic mineralization phenotype were analyzed as a whole. Ingenuity Pathway Analysis® revealed the presence of a complex and multi-branched network among 22 known genes including *Abcc6* (Figure 5, highlighted in red) and nine candidate genes (Figure 5, highlighted in green).

DISCUSSION

Using the mouse to model human disease: the presence of modifier genes for PXE in mice

Modifier effects are remarkably common in human and model organisms (Nadeau, 2001). Modifier gene research is a subject that attracted much attention representing a paradigm shift in the study of monogenic disorders, away from the influence of the primary disease-causing gene. In addition, a recent study of a large group of healthy human “controls” showed that some individuals harbor disease-causing mutations for Mendelian disorders but are disease free (Chen *et al.*, 2016). These observations point to the fundamental phenomenon – genetic modifiers are an integral part of the genetic risk landscape of essentially all monogenic disorders, including PXE. The controlled environment of inbred mice bearing the same *Abcc6* allelic mutation allows separation of environmental effects from genetics with the recognition that PXE is a complex heritable disorder at the genome, environment, and diet interface (Uitto *et al.*, 2001; Pomozi *et al.*, 2018). Characterization of four naturally occurring *Abcc6* mutant mouse inbred strains demonstrated that it was possible to exclude environmental influences and identify genetic factors that modify the disease phenotype based on marked severity differences between them.

Abcc6 was confirmed as a strong genetic determinant for ectopic mineralization

Stepwise bioinformatics analysis reduced the large QTL intervals to a total of ten candidate genes including *Abcc6*. By comparing crosses of strains that had the same or different *Abcc6* alleles, it was possible to unambiguously demonstrate that the *Abcc6* gene on Chr.7 QTL was a strong genetic determinant of ectopic mineralization in multiple organs.

Integrative bioinformatics to identify modifier genes

Geneweaver analysis minimized false discovery rate for QTLs on Chr.3 and Chr.5. We have analyzed the QTLs that are identical by descent by comparing SNP genotypes. To identify candidate genes that fell within the QTL intervals, the parental strains were screened for the presence of SNPs in the genes which might affect expression potentially modifying the PXE phenotype. Integrative functional genomics analysis, such as genes known to be associated with ectopic mineralization phenotype or interact with *Abcc6*, and genes that play a role in bone mineralization and homeostasis, facilitated identification of candidate genes. As such, nine genes fulfilled the selection criteria (Figure 4c). Although ectopic soft tissue mineralization, the hallmark of PXE, and aberrant osseous mineralization rarely observed in these mice, it is well known that the pathophysiological mechanisms underlying both are alike (Kirsch, 2006). Indeed, studies in murine and human PXE demonstrated that perturbed

osteogenic signaling is involved in the ectopic mineralization process (Hosen *et al.*, 2014). While there is no evidence that osteogenic changes are a direct consequence of ABCC6 deficiency, it is possible that genes that regulate mineral homeostasis and/or bone mineralization could contribute to the ectopic deposition of minerals in soft connective tissues.

***Car2* and *Postn* are candidate modifier genes for heart mineralization on Chr.3 QTL**

Carbonic anhydrase II (CAR2) is a member of a family of zinc metalloenzymes involved in numerous physiological and pathological processes. *CAR2* is known to be associated with ectopic mineralization in both humans and mice (Table S1). Loss-of-function mutations in the *CAR2* gene cause an autosomal recessive disorder that produces osteopetrosis, renal tubular acidosis, and cerebral calcification (Sly *et al.*, 1983), when deleted in mice causes slowly progressive vascular calcification (Spicer *et al.*, 1989). In addition, CAR2 is expressed at high levels in osteoclasts during bone resorption (Laitala and Vaananen, 1994). Periostin, encoded by *Postn*, is a highly conserved matricellular protein expressed in a broad range of tissues including the skeleton. Periostin has multifaceted role in bone homeostasis (Bonnet *et al.*, 2016). Development of *Postn* null mice elucidated the crucial role of periostin on dentinogenesis and osteogenesis (Bonnet *et al.*, 2009).

Seven genes, *Abcg3*, *Aldh2*, *Chek2*, *Dmp1*, *Hnf1a*, *Idua*, and *TTc28*, are candidate modifier genes for renal tubule mineralization on Chr.5 QTL

Abcg3 codes for ATP-binding cassette, sub-family G, member 3. *Abcg3* was selected as a candidate because of its interaction with ABCC6 in String database (Szkarczyk *et al.*, 2017). While a recent study suggested its association with arthrogryposis-renal dysfunction-cholestasis syndrome in mouse (Chai *et al.*, 2018), the function of ABCG3 relating to ectopic mineralization is not readily relevant. Aldehyde dehydrogenase 2 (ALDH2) is the enzyme that degrades and detoxifies the acetaldehyde produced by alcohol metabolism. Disruption of the *Aldh2* gene resulted in altered cortical bone structure in mice (Tsuchiya *et al.*, 2013). In addition, an association between an *ALDH2* polymorphism and osteoporosis and hip fracture has been reported (Takeshima *et al.*, 2017; Yamaguchi *et al.*, 2006).

Checkpoint kinase 2 (CHEK2) is the main effector kinase of ataxia telangiectasia mutated (ATM) and is responsible for cell cycle regulation. CHEK2 regulates renal 25-hydroxyvitamin D 1 α -hydroxylase expression thereby impacting calcium and phosphate metabolism (Fahkri *et al.*, 2015). Dentin matrix acidic phosphoprotein 1 (DMP1) is an extracellular matrix protein and a member of the small integrin binding ligand N-linked glycoprotein family. This protein, present in diverse cells of bone and tooth tissues, is critical for proper mineralization of bone and dentin. Mutations in *DMP1* cause autosomal recessive hypophosphatemia, a disease that manifests as rickets and osteomalacia, and when deleted in mice, results in a hypomineralized bone phenotype (Feng *et al.*, 2006; Feng *et al.*, 2003).

HNF1 homeobox A (HNF1A) is a member of the hepatocyte nuclear factor (HNF) family of transcription factors that regulate organ development and glucose, amino acid, and lipid homeostasis. Human mutations in *HNF1A* cause type 3 maturity-onset diabetes of the young (MODY), characterized by the onset of diabetes mellitus before the age of 25 (McDonald

and Ellard, 2013). Mice deficient in *Hnfla* showed the typical traits of the human renal Fanconi syndrome characterized by polyuria, glucosuria, aminoaciduria, phosphaturia, and bone hypomineralization (Pontoglio *et al.*, 1996). Alpha-L-iduronidase (IDUA) is a lysosomal enzyme that participates in the degradation of dermatan sulfate and heparan sulfate. Mutations in *IDUA* cause autosomal recessive mucopolysaccharidosis type I-Hurler (MPS I-H) manifesting with skeletal deformities, hearing loss, corneal clouding, heart failure and mental retardation (Scott *et al.*, 1995). The transgenic mice carrying a nonsense mutation analogous to the human p.W402X mutation in *IDUA* have loss of a-L-iduronidase activity, significant increase in glycosaminoglycan levels in multiple tissues, and increase in bone density (Wang *et al.*, 2010). Tetratricopeptide repeat domain-containing protein 28 (TTC28) is a protein required during the cell cycle for condensation of spindle midzone microtubules, formation of the mid-body, and completion of cytokinesis. Decreased bone mineral density was reported in the *Ttc28* null mice in the repository of International Mouse Phenotyping Consortium.

Most, if not all, of the null mutations in mice for these genes were made on one of the C57BL/6 substrains that are naturally resistant to develop PXE lesions. This strain background effect and non-consistent phenotyping may explain why more extensive lesions, consistent with PXE, were not reported.

Expansion of the ectopic mineralization gene network and relevance to human PXE

Functional studies in appropriate model systems are needed to validate the role of candidate modifier genes in the ectopic mineralization process when combined with *ABCC6* mutations. In fact, the dysregulated interactions between genes known to cause ectopic mineralization are encountered. Some patients with a heterozygous mutation in *GGCX* and a heterozygous mutation in *ABCC6* display PXE-like skin features, suggesting digenic inheritance for PXE and implying a role for multiple genetic factors in ectopic mineralization in general (Li *et al.*, 2009a). Therefore, studying interaction and functional networks among the 22 known and nine candidate proteins provides the opportunity to further dissect gene-gene interactions in the process of ectopic mineralization. Because of considerable synteny between the mouse and human genomes, it is likely that some if not all the genes found in mice are also applicable to humans modifying the disease phenotype, and this possibility can be tested by genotyping cohorts of patients with PXE.

MATERIALS AND METHODS

Mice and breeding

The parental strains of mice, C57BL/6J (B6), KK/HIJ (KK), and DBA/2J (D2), were obtained from The Jackson Laboratory (Bar Harbor, ME). All mice were housed on standard rodent diet (Laboratory Autoclavable Rodent Diet 5010; PMI Nutritional International, Brentwood, MO) under standard conditions at the Animal Facility of Thomas Jefferson University. All protocols were approved by the Institutional Animal Care and Use Committee of Thomas Jefferson University.

B6 or D2 females were mated with KK male mice to produce B6KKF1 and D2KKF1 progeny, respectively. These F1 females were then backcrossed to KK males to produce N2 progeny, (B6KKF1)KK and (D2KKF1)KK, respectively. All mice used for phenotyping analysis were placed at 4 weeks of age post weaning on the “acceleration diet” (Envigo, Rodent diet TD.00442, Madison, WI) which was shown to accelerate ectopic mineralization in mouse models of PXE (Li *et al.*, 2014b; Jiang and Uitto, 2012). At 12 weeks of age, mice were necropsied. A total of 384 mice had samples taken for DNA analysis (Table S2). The two backcrosses were designed to have at least 180 N2 individuals each to achieve 93% power to detect QTL with additive effects exceeding 13% of the variance using the R/qtlDesign package (Sen *et al.*, 2007).

Histopathological analysis

Muzzle, kidney, heart, eyes, and lung were collected from 468 mice and processed for histology (Table S2). Representative paraffin blocks were serially sectioned and stained with hematoxylin and eosin or Alizarin red or von Kossa for mineralization, or Periodic Acid Schiff (PAS) to localize the basement membrane using standard procedures. The severity of lesions was scored by an experienced, board-certified veterinary pathologist (JPS). The severity of tissue mineralization is based on a semi-quantitative measure of the size of the lesion in different organs (scores: 0 normal; 1 mild; 2 moderate; 3 severe; 4 extreme). Various degrees of tissue mineralization were found and representative cases were photographed to document the range in severity. Similar grading system was used in prior studies to successfully identify modifier genes for other diseases (Sundberg *et al.*, 1994; Jurisic *et al.*, 2010; Swaminathan *et al.*, 2013).

Chemical quantitation of calcium in muzzle skin

Muzzle skin biopsies were harvested and decalcified with 0.15 mol/L HCl for 48 hours at room temperature. The solubilized calcium was determined by colorimetric analysis using the α -cresolphthalein complexone method (calcium (CPC) LiquiColor; Stanbio Laboratory, Boerne, TX). The values were normalized to tissue weight.

DNA isolation and genotyping

A total of 384 samples were included in the DNA genotyping analysis (Table S2). Genomic DNA was extracted from tail tips at The Jackson Laboratory and genotyped at Geneseek using GigaMUGA SNP genotyping array (Neogen Corporation, Lincoln NE) consisting of approximately 143,000 probes.

Quantitative trait locus (QTL) analysis

All QTL analyses were performed with the R/qtl software package (<http://www.rqtl.org/>). Given each phenotype distribution we used a non-parametric model in each of the QTL analyses. For each phenotype, genome-wide significance thresholds of 0.01, 0.05, 0.10 and 0.63 were obtained following 1000 permutations. Candidate intervals for each phenotype were defined using a two LOD drop approach from the peak QTL.

GeneWeaver: Integrated search for candidate genes

The protein coding genes within the QTL confidence intervals were exported from MGI into GeneWeaver as QTL Gene Sets (GS352436, GS352533, GS352620). A set of genes was created specific to each of the tissues of interest from NCBI GEO and the primary literature (heart GS352736 (Lin *et al.*, 2014) and kidney GS352510 (Rubin *et al.*, 2016)). A set of genes was created using String database to include all known protein-protein interactions with ABCC6 (GS352441). Finally, sets of genes containing any SNPs between KK and B6/D2 (GS352512), or just cnSNPs between KK and D2 (GS352739) were created. For each QTL additional Gene Sets related to the phenotype were identified using the Search Tool in GeneWeaver from the Mammalian Phenotype Ontology or Human Phenotype Ontology Term. Figure S4 and S5 illustrate the workflow to identify candidate modifier genes. The HiSim Graph tool was subsequently run with default parameters to identify set-set overlap using the parabolic enumeration algorithm.

Gene network construction

A gene network of protein-protein and gene-regulatory interactions among the 22 known genes including *ABCC6* were built using the custom pathway functionality within the Ingenuity Pathways Analysis® software (<http://www.ingenuity.com>; QIAGEN, Redwood City, CA). First, the 22 genes were added to the network editing tool, “My Pathways”. Next, the “Connect” tool within “My Pathways” was used to connect the genes by adding direct and indirect edges that represent protein-protein and gene-regulatory interactions. As not all genes had edges to the other genes, the “Path Explorer” tool within “My Pathways” was used to add additional genes/proteins to the network so that all 22 genes had at least one edge in the network. Finally, the nine additional candidate genes from the QTL studies were added to the network and edges added using the “Connect” tool within “My Pathways”.

Statistical analyses

Linear regression and ANOVA analysis was performed using R version 3.5.1 (<http://r-project.org>). Comparisons between different sexes of mice were performed using the two-sided Kruskal-Wallis nonparametric test using SPSS version 15.0 software (SPSS, Chicago, IL). Statistical significance was assigned at $P < 0.05$.

Supplementary Material

Refer to Web version on PubMed Central for supplementary material.

ACKNOWLEDGMENTS

The authors thank Dian Wang, Joshua Kingman, Jeffrey Lamont, Wenning Qin, Linda Siracusa, Jieyu Zhang, Jingyi Zhao, Victoria E. Kennedy, and Kathleen A. Silva for their technical assistance.

Abbreviations:

Chr	chromosome
cnSNP	coding non-synonymous single nucleotide polymorphism

IMPC	International Mouse Phenotyping Consortium
KOMP	Knockout Mouse Project
PXE	pseudoxanthoma elasticum
QTL	quantitative trait locus

REFERENCES

- Belinsky MG, Kruh GD. MOAT-E (ARA) is a full-length MRP/cMOAT subfamily transporter expressed in kidney and liver. *Br J Cancer* 1999;80:1342–9. [PubMed: 10424734]
- Bergen AA, Plomp AS, Schuurman EJ, Terry S, Breuning M, Dauwerse H, et al. Mutations in *ABCC6* cause pseudoxanthoma elasticum. *Nat Genet* 2000;25:228–31. [PubMed: 10835643]
- Berndt A, Li Q, Potter CS, Liang Y, Silva KA, Kennedy V, et al. A single-nucleotide polymorphism in the *Abcc6* gene associates with connective tissue mineralization in mice similar to targeted models for pseudoxanthoma elasticum. *J Invest Dermatol* 2013;133:833–6. [PubMed: 23014343]
- Bonnet N, Standley KN, Bianchi EN, Stadelmann V, Foti M, Conway SJ, et al. The matricellular protein periostin is required for sost inhibition and the anabolic response to mechanical loading and physical activity. *J Biol Chem* 2009;284:35939–50. [PubMed: 19837663]
- Bonnet N, Garnero P, Ferrari S. Periostin action in bone. *Mol Cell Endocrinol* 2016;432:75–82. [PubMed: 26721738]
- Borst P, Varadi A, van de Wetering K. PXE, a mysterious inborn error clarified. *Trends Biochem Sci* 2019;44:125–40. [PubMed: 30446375]
- Bubier JA, Jay JJ, Baker CL, Bergeson SE, Ohno H, Metten P, et al. Identification of a QTL in *Mus musculus* for alcohol preference, withdrawal, and *Ap3m2* expression using integrative functional genomics and precision genetics. *Genetics* 2014;197:1377–93. [PubMed: 24923803]
- Cai J, Daoud R, Alqawi O, Georges E, Pelletier J, Gros P. Nucleotide binding and nucleotide hydrolysis properties of the ABC transporter MRP6 (*ABCC6*). *Biochemistry* 2002;41:8058–67. [PubMed: 12069597]
- Chai M, Su L, Hao X, Zhang M, Zheng L, Bi J, et al. Identification of genes and signaling pathways associated with arthrogryposisrenal dysfunctioncholestasis syndrome using weighted correlation network analysis. *Int J Mol Med* 2018;42:2238–46. [PubMed: 30015832]
- Chen R, Shi L, Hakenberg J, Naughton B, Sklar P, Zhang J, et al. Analysis of 589,306 genomes identifies individuals resilient to severe Mendelian childhood diseases. *Nat Biotechnol* 2016;34:531–8. [PubMed: 27065010]
- Dabisch-Ruthe M, Brock A, Kuzaj P, Issa P Charbel, Szliska C, Knabbe C, et al. Variants in genes encoding pyrophosphate metabolizing enzymes are associated with Pseudoxanthoma elasticum. *Clin Biochem* 2014;47:60–7. [PubMed: 25025693]
- Delprato A, Algeo MP, Bonheur B, Bubier JA, Lu L, Williams RW, et al. QTL and systems genetics analysis of mouse grooming and behavioral responses to novelty in an open field. *Genes Brain Behav* 2017;16:790–9. [PubMed: 28544613]
- Fahkri H, Zhang B, Fajol A, Hernando N, Elvira B, Mannheim JG, et al. Checkpoint kinase *Chk2* controls renal *Cyp27b1* expression, calcitriol formation, and calcium-phosphate metabolism. *Pflugers Arch* 2015;467:1871–80. [PubMed: 25319519]
- Feng JQ, Huang H, Lu Y, Ye L, Xie Y, Tsutsui TW, et al. The Dentin matrix protein 1 (*Dmp1*) is specifically expressed in mineralized, but not soft, tissues during development. *J Dent Res* 2003;82:776–80. [PubMed: 14514755]
- Feng JQ, Ward LM, Liu S, Lu Y, Xie Y, Yuan B, et al. Loss of *DMP1* causes rickets and osteomalacia and identifies a role for osteocytes in mineral metabolism. *Nat Genet* 2006;38:1310–5. [PubMed: 17033621]
- Gorgels TG, Hu X, Scheffer GL, van der Wal AC, Toonstra J, de Jong PT, et al. Disruption of *Abcc6* in the mouse: novel insight in the pathogenesis of pseudoxanthoma elasticum. *Hum Mol Genet* 2005;14:1763–73. [PubMed: 15888484]

- Hosen MJ, Coucke PJ, Le Saux O, De Paepe A, Vanakker OM. Perturbation of specific pro-mineralizing signalling pathways in human and murine pseudoxanthoma elasticum. *Orphanet J Rare Dis* 2014;9:66. [PubMed: 24775865]
- Ilias A, Urban Z, Seidl TL, Le Saux O, Sinko E, Boyd CD, et al. Loss of ATP-dependent transport activity in pseudoxanthoma elasticum-associated mutants of human ABCC6 (MRP6). *J Biol Chem* 2002;277:16860–7. [PubMed: 11880368]
- Iwanaga A, Okubo Y, Yozaki M, Koike Y, Kuwatsuka Y, Tomimura S, et al. Analysis of clinical symptoms and ABCC6 mutations in 76 Japanese patients with pseudoxanthoma elasticum. *J Dermatol* 2017;44:644–50. [PubMed: 28186352]
- Jiang Q, Endo M, Dibra F, Wang K, Uitto J. Pseudoxanthoma elasticum is a metabolic disease. *J Invest Dermatol* 2009;129:348–54. [PubMed: 18685618]
- Jiang Q, Oldenburg R, Otsuru S, Grand-Pierre AE, Horwitz EM, Uitto J. Parabiotic heterogenetic pairing of *Abcc6*^{-/-}/*Rag1*^{-/-} mice and their wild-type counterparts halts ectopic mineralization in a murine model of pseudoxanthoma elasticum. *Am J Pathol* 2010;176:1855–62. [PubMed: 20185580]
- Jiang Q, Uitto J. Restricting dietary magnesium accelerates ectopic connective tissue mineralization in a mouse model of pseudoxanthoma elasticum (*Abcc6*^{-/-}). *Exp Dermatol* 2012;21:694–9. [PubMed: 22897576]
- Jurisc G, Sundberg JP, Bleich A, Leiter EH, Broman KW, Buechler G, et al. Quantitative lymphatic vessel trait analysis suggests *Vcam1* as candidate modifier gene of inflammatory bowel disease. *Genes Immun* 2010;11:219–31. [PubMed: 20220769]
- Kirsch T Determinants of pathological mineralization. *Curr Opin Rheumatol* 2006;18:174–80. [PubMed: 16462525]
- Klement JF, Matsuzaki Y, Jiang QJ, Terlizzi J, Choi HY, Fujimoto N, et al. Targeted ablation of the *Abcc6* gene results in ectopic mineralization of connective tissues. *Mol Cell Biol* 2005;25:8299–310. [PubMed: 16135817]
- Laitala T, Vaananen HK. Inhibition of bone resorption in vitro by antisense RNA and DNA molecules targeted against carbonic anhydrase II or two subunits of vacuolar H(+)-ATPase. *J Clin Invest* 1994;93:2311–8. [PubMed: 8200964]
- Le Boulanger G, Labreze C, Croue A, Schurgers LJ, Chassaing N, Wittkamp T, et al. An unusual severe vascular case of pseudoxanthoma elasticum presenting as generalized arterial calcification of infancy. *Am J Med Genet A* 2010;152A:118–23. [PubMed: 20034067]
- Le Saux O, Urban Z, Tschuch C, Csiszar K, Bacchelli B, Quaglino D, et al. Mutations in a gene encoding an ABC transporter cause pseudoxanthoma elasticum. *Nat Genet* 2000;25:223–7. [PubMed: 10835642]
- Legrand A, Cornez L, Samkari W, Mazzella JM, Venisse A, Boccio V, et al. Mutation spectrum in the ABCC6 gene and genotype-phenotype correlations in a French cohort with pseudoxanthoma elasticum. *Genet Med* 2017;19:909–17. [PubMed: 28102862]
- Li Q, Grange DK, Armstrong NL, Whelan AJ, Hurley MY, Rishavy MA, et al. Mutations in the *GGCX* and *ABCC6* genes in a family with pseudoxanthoma elasticum-like phenotypes. *J Invest Dermatol* 2009a;129:553–63. [PubMed: 18800149]
- Li Q, Jiang Q, Pfendner E, Varadi A, Uitto J. Pseudoxanthoma elasticum: clinical phenotypes, molecular genetics and putative pathomechanisms. *Exp Dermatol* 2009b;18:1–11. [PubMed: 19054062]
- Li Q, Berndt A, Guo H, Sundberg J, Uitto J. A novel animal model for pseudoxanthoma elasticum - the KK/HIJ mouse. *Am J Pathol* 2012;181:1190–6. [PubMed: 22846719]
- Li Q, Brodsky JL, Conlin L, Pawel B, Glatz A, Gafni RI, et al. Mutations in the *ABCC6* gene as a cause of generalized arterial calcification of infancy: Genotypic overlap with pseudoxanthoma elasticum. *J Invest Dermatol* 2014a;134:658–65. [PubMed: 24008425]
- Li Q, Guo H, Chou DW, Berndt A, Sundberg JP, Uitto J. Mouse models for pseudoxanthoma elasticum: genetic and dietary modulation of the ectopic mineralization phenotypes. *PLoS One* 2014b;9:e89268. [PubMed: 24586646]

- Li Q, Kingman J, van de Wetering K, Tannouri S, Sundberg JP, Uitto J. Abcc6 knockout rat model highlights the role of liver in PPI homeostasis in pseudoxanthoma elasticum. *J Invest Dermatol* 2017;137:1025–32. [PubMed: 28111129]
- Li Q, van de Wetering K, Uitto J. Pseudoxanthoma elasticum as a paradigm of heritable ectopic mineralization disorders: Pathomechanisms and treatment development. *Am J Pathol* 2019;189:216–25. [PubMed: 30414410]
- Lin S, Lin Y, Nery JR, Urich MA, Breschi A, Davis CA, et al. Comparison of the transcriptional landscapes between human and mouse tissues. *Proc Natl Acad Sci U S A* 2014;111:17224–9. [PubMed: 25413365]
- McDonald TJ, Ellard S. Maturity onset diabetes of the young: identification and diagnosis. *Ann Clin Biochem* 2013;50:403–15. [PubMed: 23878349]
- Nadeau JH. Modifier genes in mice and humans. *Nat Rev Genet* 2001;2:165–74. [PubMed: 11256068]
- Neldner KH. Pseudoxanthoma elasticum. *Clin Dermatol* 1988;6:1–159.
- Nitschke Y, Baujat G, Botschen U, Wittkampf T, Moulin M du, Stella J, et al. Generalized arterial calcification of infancy and pseudoxanthoma elasticum can be caused by mutations in either *ENPP1* or *ABCC6*. *Am J Hum Genet* 2012;90:25–39. [PubMed: 22209248]
- Nitschke Y, Rutsch F. Genetics in arterial calcification: lessons learned from rare diseases. *Trends Cardiovasc Med* 2012;22:145–9. [PubMed: 23122642]
- Pfendner EG, Vanakker OM, Terry SF, Vourthis S, McAndrew PE, McClain MR, et al. Mutation detection in the *ABCC6* gene and genotype-phenotype analysis in a large international case series affected by pseudoxanthoma elasticum. *J Med Genet* 2007;44:621–8. [PubMed: 17617515]
- Pomozi V, Julian CB, Zoll J, Pham K, Kuo S, Tokesi N, et al. Dietary pyrophosphate modulates calcification in a mouse model of pseudoxanthoma elasticum: Implication for treatment of patients. *J Invest Dermatol* 2018;10.1016/j.jid.2018.10.040.
- Pontoglio M, Barra J, Hadchouel M, Doyen A, Kress C, Bach JP, et al. Hepatocyte nuclear factor 1 inactivation results in hepatic dysfunction, phenylketonuria, and renal Fanconi syndrome. *Cell* 1996;84:575–85. [PubMed: 8598044]
- Ringpfeil F, Lebowitz MG, Christiano AM, Uitto J. Pseudoxanthoma elasticum: mutations in the MRP6 gene encoding a transmembrane ATP-binding cassette (ABC) transporter. *Proc Natl Acad Sci U S A* 2000;97:6001–6. [PubMed: 10811882]
- Rubin A, Salzberg AC, Imamura Y, Grivtishvilli A, Tombran-Tink J. Identification of novel targets of diabetic nephropathy and PEDF peptide treatment using RNA-seq. *BMC Genomics* 2016;17:936. [PubMed: 27855634]
- Rutsch F, Ruf N, Vaingankar S, Toliat MR, Suk A, Hohne W, et al. Mutations in ENPP1 are associated with ‘idiopathic’ infantile arterial calcification. *Nature Genet* 2003;34:379–81. [PubMed: 12881724]
- Scheffer GL, Hu X, Pijnenborg AC, Wijnholds J, Bergen AA, Scheper RJ. MRP6 (ABCC6) detection in normal human tissues and tumors. *Lab Invest* 2002;82:515–8. [PubMed: 11950908]
- Scott HS, Bunge S, Gal A, Clarke LA, Morris CP, Hopwood JJ. Molecular genetics of mucopolysaccharidosis type I: diagnostic, clinical, and biological implications. *Hum Mutat* 1995;6:288–302. [PubMed: 8680403]
- Sen S, Satagopan JM, Broman KW, Churchill GA. R/qtlDesign: inbred line cross experimental design. *Mamm Genome* 2007;18:87–93. [PubMed: 17347894]
- Sly WS, Hewett-Emmett D, Whyte MP, Yu YS, Tashian RE. Carbonic anhydrase II deficiency identified as the primary defect in the autosomal recessive syndrome of osteopetrosis with renal tubular acidosis and cerebral calcification. *Proc Natl Acad Sci U S A* 1983;80:2752–6. [PubMed: 6405388]
- Spicer SS, Lewis SE, Tashian RE, Schulte BA. Mice carrying a CAR-2 null allele lack carbonic anhydrase II immunohistochemically and show vascular calcification. *Am J Pathol* 1989;134:947–54. [PubMed: 2495727]
- Sundberg JP, Elson CO, Bedigian H, Birkenmeier EH. Spontaneous, heritable colitis in a new substrain of C3H/HeJ mice. *Gastroenterology* 1994;107:1726–35. [PubMed: 7958684]

- Sundberg JP, Berndt A, Sundberg BA, Silva KA, Kennedy V, Bronson R, et al. The mouse as a model for understanding chronic diseases of aging: The histopathologic basis of aging in inbred mice. *Pathobiol Aging Age Relat Dis* 2011;1.
- Swaminathan S, Lu H, Williams RW, Lu L, Jablonski MM. Genetic modulation of the iris transillumination defect: a systems genetics analysis using the expanded family of BXD glaucoma strains. *Pigment Cell Melanoma Res* 2013;26:487–98. [PubMed: 23582180]
- Szklarczyk D, Morris JH, Cook H, Kuhn M, Wyder S, Simonovic M, et al. The STRING database in 2017: quality-controlled protein-protein association networks, made broadly accessible. *Nucleic Acids Res* 2017;45:D362–D8. [PubMed: 27924014]
- Takeshima K, Nishiwaki Y, Suda Y, Niki Y, Sato Y, Kobayashi T, et al. A missense single nucleotide polymorphism in the ALDH2 gene, rs671, is associated with hip fracture. *Sci Rep* 2017;7:428. [PubMed: 28348376]
- Tsuchiya T, Sakai A, Menuki K, Mori T, Takeuchi Y, Kanoh S, et al. Disruption of aldehyde dehydrogenase 2 gene results in altered cortical bone structure and increased cortical bone mineral density in the femoral diaphysis of mice. *Bone* 2013;53:358–68. [PubMed: 23313283]
- Uitto J, Pulkkinen L, Ringpfeil F. Molecular genetics of pseudoxanthoma elasticum: a metabolic disorder at the environment-genome interface? *Trends Mol Med* 2001;7:13–7. [PubMed: 11427982]
- Uitto J, Li Q, van de Wetering K, Varadi A, Terry SF. Insights into pathomechanisms and treatment development in heritable ectopic mineralization disorders: Summary of the PXE International Biennial Research Symposium-2016. *J Invest Dermatol* 2017;137:790–5. [PubMed: 28340679]
- Wang D, Shukla C, Liu X, Schoeb TR, Clarke LA, Bedwell DM, et al. Characterization of an MPS I-H knock-in mouse that carries a nonsense mutation analogous to the human IDUA-W402X mutation. *Mol Genet Metab* 2010;99:62–71. [PubMed: 19751987]
- Yamaguchi J, Hasegawa Y, Kawasaki M, Masui T, Kanoh T, Ishiguro N, et al. ALDH2 polymorphisms and bone mineral density in an elderly Japanese population. *Osteoporos Int* 2006;17:908–13. [PubMed: 16520888]

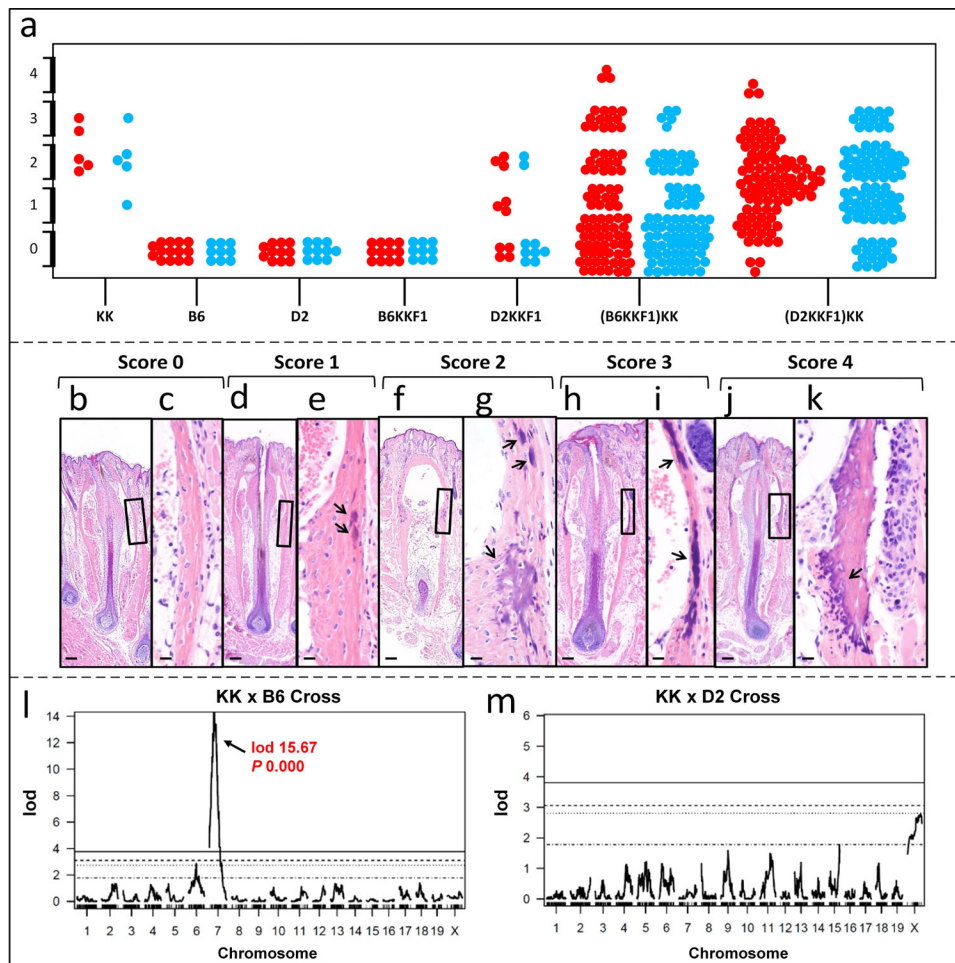


Figure 1. Histopathology of vibrissae mineralization in muzzle skin and QTL plots.

(a), Phenotypic scores of the parental strains of mice, F1 and N2 progeny determined by histopathology. Each dot represents a mouse (red, females; blue, males). Only the D2KKF1 hybrid mice differed with sex as female mice had higher severity than males (Chi-square 19.73, $P = 0.0006$). (b-k), Histopathological evaluation of ectopic mineralization. Vertical sections of vibrissae had no evidence of mineralization in the connective tissue sheath or outer root sheath (b, score 0; c, enlarged boxed area in d). Mild mineralization was when one or two follicles had faintly evident mineralization in the connective tissue sheath (d, score 1; e, enlarged boxed area in d). Moderate had one or two follicles with obvious but not extensive mineralization (f, score 2; g, enlarged boxed area in f). Severe cases had multiple follicles affected with prominent mineralization (h, score 3; i, enlarged boxed area in h). Extreme cases had extensive mineralization often with granuloma formation at the site of mineralization (j, score 4; k, enlarged boxed area in j). Ectopic mineralization is indicated by arrows. Scale bar = 100 μm (panels b, d, f, h, and j). Scale bar = 20 μm (panels c, e, g, I, and k). (l-m), QTL plots from KK x B6 and KK x D2 crosses. KK and D2 both have the *Abcc6* mutant allele while B6 has the wild type allele. Therefore, in KK x B6 cross, a major QTL was identified on Chr. 7 that involves *Abcc6* ($P < 0.05$); however, there is no linkage to *Abcc6* in KK x D2 cross.

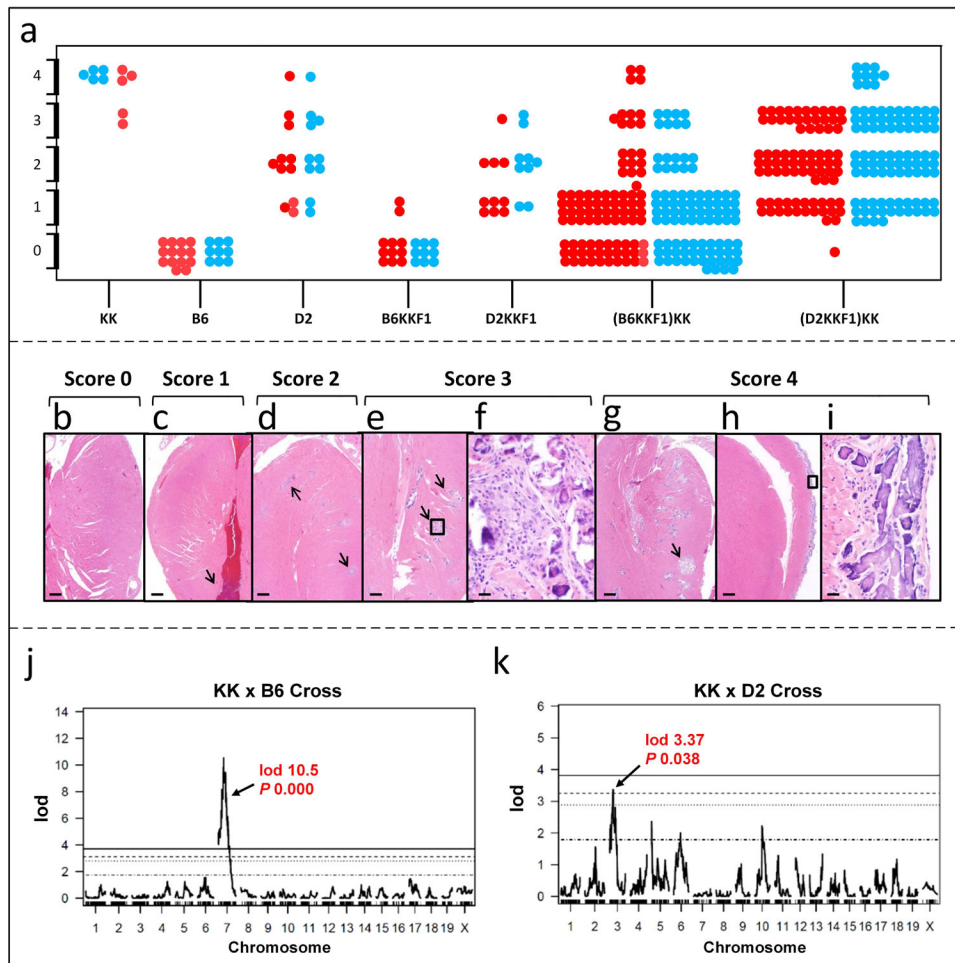


Figure 2. Histopathology of heart mineralization and QTL plots.

(a), Phenotypic scores of the parental strains of mice, F1 and N2 progeny determined by histopathology. Each dot represents a mouse (red, females; blue, males). (b-i), Histopathologic evaluation of ectopic mineralization. The heart in a few mice was normal (b, score 0); however most had small focal lesions of mineralization within the myocardium (c, score 1), small but multiple areas of mineralization with some degree of fibrosis (d, score 2), extensive areas (e, score 3), or very large and extensive areas (g, score 4). Epicardial mineralization and fibrosis, the more common presentation of dystrophic cardiac calcinosis in inbred strains of mice, was relatively infrequent (h). Enlargement of the boxed area in h illustrates the prominent mineralization with some fibrosis and infiltration with macrophages (i). The myocardial mineralization usually contained a variety of inflammatory cells, mostly macrophages, in the moderate to severe forms (f, enlargement of boxed area in e). Ectopic mineralization is indicated by arrows. Scale bar = 500 μ m (panels b, c, d, e, g, and h). Scale bar = 20 μ m (panels f and i). (j-k), QTL plots from KK x B6 and KK x D2 crosses. KK and D2 both have the *Abcc6* mutant allele while B6 has the wild type allele. Therefore, in KK x B6 cross, a major QTL was identified on Chr. 7 that involves *Abcc6* ($P < 0.05$); however, there is no linkage to *Abcc6* in KK x D2 cross. In addition, a QTL on Chr. 3 was identified in KK x D2 cross.

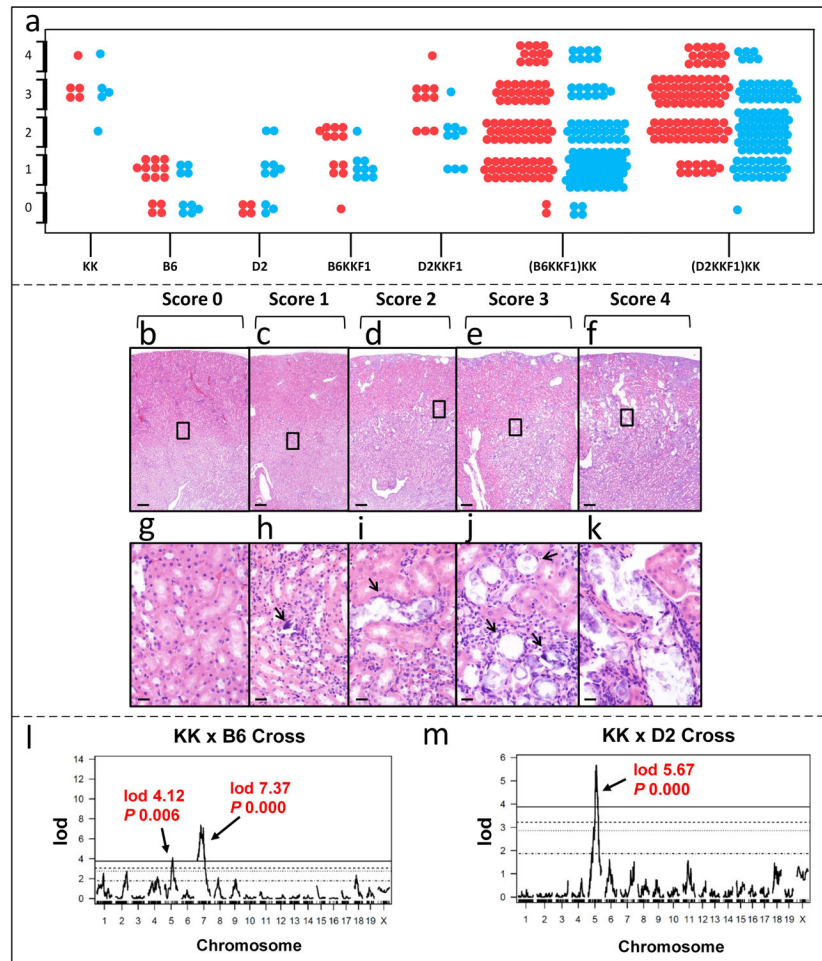


Figure 3. Histopathology of kidney mineralization and QTL plots.

(a), Phenotypic scores of the parental strains of mice, F1 and N2 progeny determined by histopathology. Each dot represents a mouse (red, females; blue, males). Kidney mineralization phenotypes were more severe in female mice in B6KKF1 (Chi-square 6.54, $P = 0.038$), D2KKF1 (Chi-square 8.04, $P = 0.045$), (B6KKF1)KK (Chi-square 9.83, $P = 0.044$) and (D2KKF1)KK (Chi-square 14.73, $P = 0.005$) hybrid mice. (b-k), Histopathologic evaluation of ectopic mineralization. Normal kidneys were infrequent in the backcrossed mice (b, score 0). Mild cases of renal tubular mineralization consisted of occasional mineralized foci within tubules (c, score 1). Moderate cases had numerous scattered mineral filled tubules (d, score 2). Severe had many affected tubules, especially in the medulla, but none or few tubules were markedly dilated (e, score 3). Extremely severe cases involved many tubules in both the cortex and medulla with marked dilation of the tubules filled with artifactually fragmented mineral crystals (f, score 4). Note the wedge shaped depression and basophilic staining of regenerating tubules within an area that presumably was infarcted earlier. As can be noted in the panels such areas were infrequent in mild cases and progressively increased in severity often in parallel to the degree of renal tubular mineralization. g, h, i, j and k: enlarged boxed areas of b, c, d, e and f, respectively. Ectopic mineralization is indicated by arrows. Scale bar = 200 μm (panels b-f). Scale bar = 20 μm (panels g-k). (l-m), QTL plots from KK x B6 and KK x D2 crosses. KK and D2 both have

the *Abcc6* mutant allele while B6 has the wild type allele. Therefore, in KK x B6 cross, a major QTL was identified on Chr. 7 that involves *Abcc6* ($P < 0.05$); however, there is no linkage to *Abcc6* in KK x D2 cross. In addition, a QTL on Chr. 5 was identified in both crosses.

Author Manuscript

Author Manuscript

Author Manuscript

Author Manuscript

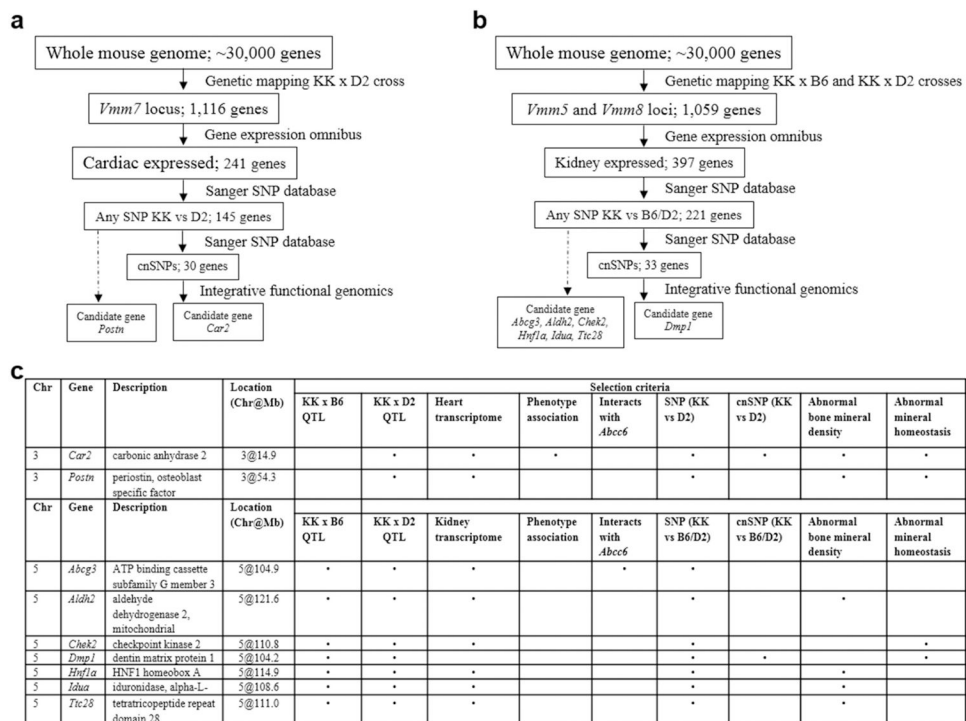


Figure 4. Schematic representation of how GeneWeaver was used to prioritize the QTL intervals, using heterogeneous data from various sources.

(a,b), The application of genetic mapping technique combined with integrative functional genomics facilitated the identification of candidate genes modifying ectopic mineralization. The details of integrative functional genomics data related to bone mineralization and homeostasis are the following: *Car2* - Mammalian Phenotype Ontology Annotation - Abnormal bone mineral density and Abnormal mineral homeostasis (KOMP phenotyping of C57BL/6-*Car2^{tm1(KOMP)Vlcg/J}*; (Spicer *et al.*, 1989)); *Postn* - Mammalian Phenotype Ontology Annotation - Abnormal bone mineral density and Abnormal mineral homeostasis (IMPC phenotyping of C57BL/6N-*Postn^{tm1.1(KOMP)Vlcg}*; (Bonnet *et al.*, 2009)); *Abcg3* - *Abcc6* interacting gene from String database (Evidence of co-expression, co-occurring in PubMed abstracts and experimental evidence of putative homologs interacting in *S.cerevisiae*); *Aldh2* - Mammalian Phenotype Ontology Annotation - Abnormal bone mineral density (IMPC phenotyping of C57BL/6N-*Aldh2^{tm1a(EUCOMM)Wtsi/Jeg}*; (Tsuchiya *et al.*, 2013)); *Chek2* - Mammalian Phenotype Ontology Annotation - Abnormal mineral homeostasis (IMPC phenotyping of C57BL/6N-*Chek2^{tm1b(EUCOMM)Hmgu/J}*; (Fahkri *et al.*, 2015)); *Dmp1* - Mammalian Phenotype Ontology Annotation - Abnormal bone mineral density (Feng *et al.*, 2003; Feng *et al.*, 2006); *Hnf1a* - Mammalian Phenotype Ontology Annotation - Abnormal bone mineral density (Pontoglio *et al.*, 1996); *Idua* - Mammalian Phenotype Ontology Annotation - Abnormal bone mineral density (Wang *et al.*, 2010); *Ttc28* - Mammalian Phenotype Ontology Annotation - Abnormal bone mineral density (IMPC phenotyping of C57BL/6N-*Ttc28^{tm1b(EUCOMM)Hmgu/Tcp}*). Chr, Chromosome. cnSNP, coding non-synonymous single nucleotide polymorphism; IMPC, International Mouse Phenotyping Consortium. KOMP, Knockout Mouse Project. QTL, quantitative trait

locus. (c), Summary of the candidate modifier genes from Geneweaver analysis. For detailed stepwise hierarchical illustrations, see Fig. S4 and Fig. S5.

Author Manuscript

Author Manuscript

Author Manuscript

Author Manuscript

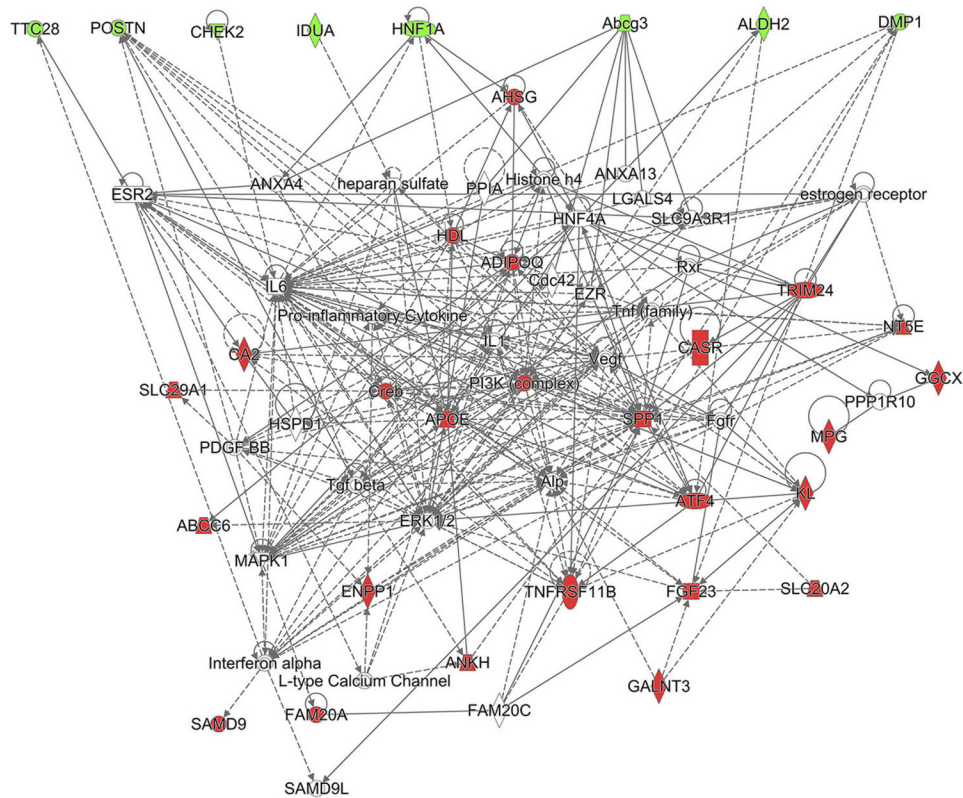


Figure 5. Complex ectopic mineralization gene network.

Twenty-two genes from Table S1 associated with ectopic mineralization (highlighted in red) and nine candidate genes (highlighted in green) linked by direct (solid lines) and indirect (dashed line) protein-protein and gene regulatory interactions using Ingenuity Pathways Analysis. Note that the mouse does not have the corresponding ortholog of human *SAMD9* gene and human do not have an ortholog of mouse *Abcg3*. *Alp* is the same gene as *ALPL* which encodes tissue non-specific alkaline phosphatase.

Table 1.

All statistically significant QTLs in the two backcross studies

Organ	KK x B6 cross					KK x D2 cross				
	Chr	LOD	QTL	Pval	Chr Interval (Mbp)*	Chr	LOD	QTL	Pval	Chr Interval (Mbp)*
Muzzle	7	15.67	<i>Vmm1</i>	0.000	47.5 – 56.9					
Heart	7	10.50	<i>Vmm2</i>	0.000	47.5 – 74.5	3	3.37	<i>Vmm7</i>	0.038	13.5 – 76.3
Lung	7	3.64	<i>Vmm3</i>	0.006	37.6 – 72.4					
Kidney	7	7.37	<i>Vmm4</i>	0.000	37.6 – 87.4					
	5	4.12	<i>Vmm5</i>	0.006	76.9 – 125.3	5	5.67	<i>Vmm8</i>	0.000	97.9 – 128.3
Eye	7	6.11	<i>Vmm6</i>	0.000	62.2 – 103.1					

*95% confidence interval.

Author Manuscript

Author Manuscript

Author Manuscript

Author Manuscript